Preparation and antioxidant activity of albumin binding Salen Schiff-base metal complexes

LI Gang[1,2], ZHANG HuiFang[1], WANG RongMin[1*], HE YuFeng[1] & XIONG YuBing[1]

[1] *Key Laboratory of Eco-Environment-Related Polymer Materials of Ministry of Education, Key Laboratory of Polymer Materials of Gansu Province, Institute of Polymer, Northwest Normal University, Lanzhou 730070, China;*
[2] *Lanzhou Institute of Biological Products, Lanzhou 730046, China*

A kind of novel biopolymer antioxidant (BSA/HOSalenM, M=Co, Mn, Zn) is prepared with conjugation, which increases the antioxidant activity of the bovine serum albumin (BSA). The conjugations have been characterized by IR spectra, UV-Vis spectra, Fluorescence spectra, Circular dichroism (CD) spectra and Native-PAGE. The BSA is used as a biopolymer scaffold, and the insoluble Salen Schiff-base metal complexes HOSalenM make axial coordination with the amino acid residues of the BSA. The structure of the BSA is unchanged when the binding rate of HOSalenCo is less than 10. The HOSalenCo conjugations show an excellent hydroxyl radical ($\cdot$OH) scavenging activity, and the activity (EC_{50}) of BSA/HOSalenCo(10) (BSA : HOSalenCo=1 : 10) is improved by two orders of magnitude compared with the BSA, while the activity of the BSA/HOSalenMn is weak and the BSA/HOSalenZn shows no scavenging activity.

bovine serum albumin, Schiff-base metal complexes, biopolymer metal complexes, hydroxyl radical scavenging activity

The reactive oxygen species (ROSs) are associated with the carcinogenesis, the coronary heart disease and many health problems which are related to advancing age [1–3]. The hydroxyl radical ($\cdot$OH) is one of the most damaging radicals produced under the physiological conditions. Epidemiological and clinical studies indicate that the effective antioxidants can protect the human body from the free radicals and retard the progress of many chronic diseases [4,5]. Many ROS-scavenging materials, including natural and synthetic antioxidants, are used to reduce the damage to the human body [6,7]. As synthetic antioxidants, Schiff-base metal complexes have been widely studied as the effective scavengers of the ROS [8–11]. However, the majority of Schiff-base metal complexes are insoluble in the aqueous solutions, which limits their applications.

The serum albumin is a versatile protein, principally characterized by its remarkable ability of binding a wide range of insoluble endogenous and exogenous compounds [12–15]. Since the serum albumin was considered to be non-antigenic and biodegradable, and was readily available [16], the albumin has been used as a bio-material, such as drug delivery and novel hydrophilic carriers [17–20]. However, the bovine serum albumin (BSA) has not been used for ROS-scavenging materials because the ROS-scavenging activity of the BSA is very weak [21]. Recently, the macromolecules conjugation has been proved to be an effective method to improve their bioactivity [22]. In this paper, a biopolymer BSA and Salen Schiff-base metal complexes were integrated together, which afforded a new kind of water-soluble biopolymer conjugation. The specific affinity between the small molecule and the protein was proved to be one of the most straightforward and applicable approaches

*Corresponding author (email: wangrm@nwnu.edu.cn)

in the enzyme mimics field.

1 Materials and methods

1.1 Materials and techniques

The BSA used here was from Shanghai Sangon Biological Engineering Technology & Services Co. Ltd, 4-hydroxyl salicylaldehyde and 1,2-ethylenediamine from Shanghai Institute of Biological Products, *n*-propylalcohol from Tianjin Chemical Reagent, $Co(OAc)_2 \cdot 2H_2O$, $Zn(OAc)_2 \cdot 2H_2O$ and $Mn(OAc)_2 \cdot 4H_2O$ from Shanghai Zhenxin Chemical Reagent Factory, $Co(OAc)_2 \cdot 4H_2O$ from Beijing Shuanghuan Weiye Reagent Co. Ltd, and Dimethylsolfuxide (DMSO) from BASF Tianjin Group. Other chemicals were of analytical reagent grade and used without further purification. The Schiff-base solutions were prepared in DMSO and the BSA solutions were prepared in the sodium phosphate buffer solution (PBS, pH 7.4). The double-distilled water was used throughout.

1.2 Preparation of Salen Schiff-base ligand and its complexes

The Salen Schiff-base ligand (HOSalen) was synthesized according to the traditional method [23], from the condensation of 1,2-ethylenediamine with 4-hydroxyl salicylaldehyde in a molar ratio of 1:2, using the *n*-propylalcohol as a solvent. Then the HOSalen was dried under vacuum and characterized by IR, UV-Vis spectra, and HNMR spectra. The spectra data are as follows: ^1H NMR spectra (DMSO-d6): 3.91 (4H, m, $-CH_2$), 6.2–7.15 (6H, m, Ar–H), 8.33 (2H, s, $-CH=N$). UV-Vis spectra: 216 nm (K band), 330 nm (R band). IR (KBr): 1639 cm^{-1} ($\nu_{C=N}$), 1234 cm^{-1} ($\nu_{Ph\text{-}O}$).

The Salen Schiff-base Cobalt complex (HOSalenCo) was prepared as follows. The solution of HOSalen/DMSO was stirred at 70°C for 15 min. Then the aqueous solution of $Co(OAc)_2 \cdot 4H_2O$ was added with a molar ratio of 1:10. The reaction mixture was stirred at 70°C for 5 h under the nitrogen atmosphere. After cooling to the room temperature, the products were filtered and washed using *n*-propanol for three times. Then the HOSalenCo was dried in the vacuum condition. The UV-Vis spectra showed K band and R band appeared at 216 and 320 nm, respectively. The IR spectra appeared at 1606 cm^{-1} ($\nu_{C=N}$), 1227 cm^{-1} ($\nu_{Ph\text{-}O}$), 465 cm^{-1} ($\nu_{Co\text{-}O}$) and 662 cm^{-1} ($\nu_{Co\text{-}N}$).

The preparations of the HOSalenMn and HOSalenZn were the same as that of the HOSalenCo except that $Mn(OAc)_2 \cdot 4H_2O/Zn(OAc)_2 \cdot 2H_2O$ was added to the reaction mixture. In the HOSalenMn, the UV-Vis spectra of K band and R band were 220 and 333 nm respectively, and the IR spectra appeared at 1641 cm^{-1} ($\nu_{C=N}$), 1234 cm^{-1} ($\nu_{Ph\text{-}O}$), 459 cm^{-1} ($\nu_{Mn\text{-}O}$), and 610 cm^{-1} ($\nu_{Mn\text{-}N}$). In the HOSalenZn, the UV-Vis spectra of K band and R band were appeared at 216

and 330 nm respectively, and the IR spectra appeared at 1602 cm^{-1} ($\nu_{C=N}$), 1219 cm^{-1} ($\nu_{Ph\text{-}O}$), 467 cm^{-1} ($\nu_{Zn\text{-}O}$), and 610 cm^{-1} ($\nu_{Zn\text{-}N}$).

1.3 Preparation of BSA conjugated Schiff-base complexes (BSA/HOSalenCo)

Firstly, the BSA was dissolved in 10 mL of PBS and the HOSalenCo was dissolved in the DMSO. Then 0.5 mL of BSA solution (1 mmol/L) and 0.228 mL of HOSalenCo (4.4 mmol/L) were added to 3.0 mL of PBS (HOSalenCo:BSA= 2:1). The mixture was incubated for 12 h with rotation in dark at room temperature. Then the complex was dialyzed in the PBS to remove the unreacted HOSalenCo and DMSO at 5–10°C. When the ratio of the HOSalenCo to the BSA was 2:1, the prepared complex was called BSA/HOSalenCo (2). In this way, BSA/HOSalenCo (20), BSA/HOSalenCo (10), and BSA/HOSalenCo (5) represented that the added ratios of HOSalenCo to BSA were 20:1, 10:1, and 5:1, respectively. After dialyzing, the concentrations of BSA/HOSalenCo complexes were calculated based on the final concentration of the BSA.

The preparations of BSA/HOSalenZn and BSA/HO-SalenMn were similar to that of BSA/HOSalenCo by conjugating action between the BSA and the HOSalenMn or HOSalenZn. However, the binding capacity of the HOSalenMn and HOSalenZn with the BSA was very weak. In dialyzing, the unconjugated HOSalphenMn and HOSalphenZn were removed. UV-Vis spectra showed the binding value of the HOSalenMn in the BSA/HOSalenMn(20) was 0.5 and the HOSalenZn in the BSA/HOSalenZn(20) was 1.5.

1.4 Scavenging ability for hydroxyl radical

The scavenging activity for ·OH was measured by the Phen-Fe^{2+} reaction [24]. The ·OH produced in the system was tested through the absorbance change at 510 nm by the UV-Vis spectra. The total volume of the reaction mixture was 5 mL including 2.0 mL of PBS (100 mmol/L), 0.2 mL of orthophenanthroline (7.5 mmol/L), 0.2 mL of $FeSO_4$ (7.5 mmol/L), 1.0 mL of H_2O_2 (0.1%) and prepared samples (BSA/SalenM). The tube which was added with PBS instead of H_2O_2 was used as the control group. After the mixture was incubated at 37°C for 60 min, the absorbance of the mixture was measured at 510 nm by a spectrophotometer. The ·OH scavenging activity was calculated according to the following equation.

$$\text{Scavenging activity} = (A_2 - A_1 / A_0 - A_1) \times 100\%,$$

where A_0 was the absorbance of the control group (PBS, orthophenanthroline, $FeSO_4$), A_1 was the absorbance for the absence of the BSA/SalenM (PBS, orthophenanthroline, $FeSO_4$, H_2O_2), and A_2 was the absorbance for the presence

of the antioxidant (PBS, Orthophenanthroline, FeSO$_4$, H$_2$O$_2$, BSA/SalenM).

2   Results and discussions

The BSA was used as the scaffold here for several reasons. Firstly, the BSA was a major soluble protein in the circulatory system and the most outstanding property of the albumins was the ability of binding endogenous and exogenous compounds. Secondly, the BSA acted as a model protein in the study of binding small molecule because the structure of the BSA was similar to the human serum albumin (HSA), which was water-soluble and had at least three specific binding sites for the hydrophobic substance. Thirdly, there were hydrophilic and hydrophobic areas in the BSA. The BSA was water-soluble but it had hydrophobic cavities. The hydrophobic substances can enter into the cavities and be integrated with the BSA. For these features, the BSA was one of the most important biopolymer materials.

2.1   UV-Vis spectra of BSA/HOSalenCo

The conjugation of BSA and metal complexes was characterized by UV-Vis spectra (Figure 1). Before conjugation, the characteristic absorption peak of BSA appeared at 280 nm. The characteristic peaks of the HOSalenCo appeared at 260 nm and 300–500 nm. However, after conjugation, the characteristic absorption peak of the BSA/HOSalenCo moved redshift. The characteristic peaks of the HOSalenCo which were at 264 and 350 nm were shifted to 266 and 363 nm, respectively. A new absorption peak appeared at 300–500 nm in the BSA/HOSalenCo compared with the BSA. It showed that the HOSalenCo was inserted into the BSA and the BSA/HOSalenCo was successfully prepared.

The binding amount of the HOSalenM (M=Co, Mn, Zn) to the BSA was confirmed by the UV-Vis spectra. After the HOSalenCo was conjugated with the BSA, the absorption peak of the HOSalenCo did not change at 370 nm (Figure 1). Therefore, the peak at 370 nm was employed to measure the binding amount in BSA/HOSalenCo. It showed that the binding amounts of HOSalenCo in BSA/HOSalenCo (20), BSA/HOSalenCo (10), BSA/HOSalenCo (5) and BSA/HOSalenCo (2) were 16, 10, 5 and 2, respectively. That meant the maximal binding amount for HOSalenCo in the BSA was 16∶1. When the ratio of the HOSalenCo to the BSA was lower than 16, all HOSalenCo were integrated with the BSA.

The binding mode of the BSA/HOSalenCo was also investigated with the UV-Vis spectra. In both the HOSalenCo and HOSalen methanol solutions, the excessive 1-methylimidazole (MeIm) was added. It showed that the R band of cobalt complexes (HOSalenCo) moved redshift from 325 to 340 nm after adding MeIm. That meant there was electronic transition in N atom of HOSalenCo/MeIm. On the contrary, the absorption band of the ligand system (HOSalen/MeIm) didn't change (Figure 2) as there was no metal ion. Therefore, the centre Co^{II} ion plays an important role in the reaction and the most possible reaction mode between the HOSalenCo and MeIm was the coordination reaction by Co and N atom. Compared with the HOSalenCo/MeIm, the BSA/HOSalenCo aqueous solution exhibited the same spectral feature, i.e. the R band moved redshift from 350 to 363 nm. The similar results had also been confirmed by published results, such as r-HSA/ZnPP [20], r-HSA/Iron protoporphyrin IX system [25]. The BSA owned 17 histidines in its primary structure (GenBank: CAA76847.1). While the maximal binding ability for HOSalenCo in the BSA was 1∶16, the binding ability for HOSalenCo in the BSA was nearly the same to that of the histidines in the BSA. Therefore, we confirmed that the HOSalenCo was integrated with the BSA by the axial coordination of HOSalenCo and the histidine residues of the BSA. The conjugation process of the BSA/HoSalenCo was completed in the following two steps. Firstly, the insoluble HOSalenCo entered into the
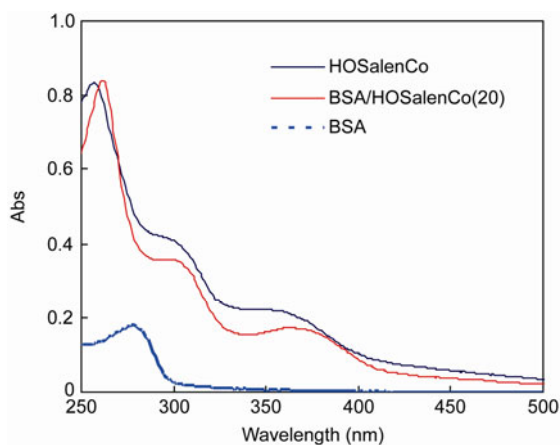

Figure 1 UV-Vis spectra of BSA, HOSalenCo and BSA/HOSalenCo (BSA/HOSalenCo=2.0×10^{-6} mol/L, HOSalenCo=1.6×10^{-6} mol/L).
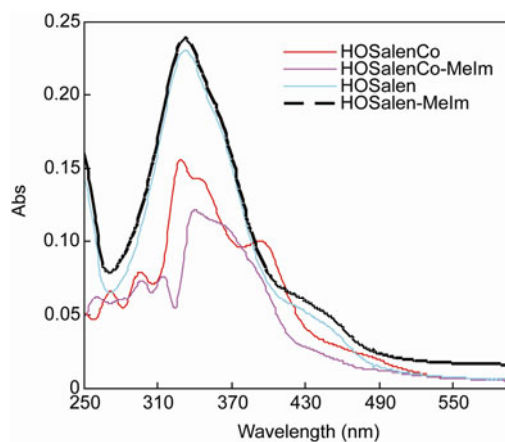

Figure 2 UV-Vis spectra of HOSalenCo, HOSalenCo/MeIm, HOSalen, and HOSalen/MeIm. (HOSalenCo=1.2×10^{-6} mol/L, HOSalen=2.0×10^{-6} mol/L).

hydrophobic cavities of the BSA based on the hydrophobic interaction. Secondly, HOSalenCo was axially coordinated with the amino acid residues of the BSA.

2.2   Fluorescence spectra of BSA/HOSalenCo

The fluorescence quenching of the tryptophan residues in the BSA was used to detect the conjugation of the BSA/ HOSalenCo. In fluorescence spectra, the BSA showed an obvious peak at 349 nm, but the HOSalenCo did not have any fluorescent emission. The fluorescence spectra of the BSA changed when the HOSalenCo was added into the BSA (Figure 3). The fluorescence intensity of the BSA was decreased as the HOSalenCo concentration increased (Figure 3). The HSA had the similar results (Figure 4), and the fluorescence quench curve of the BSA was accordant with that of HSA.

The fluorescence of the serum albumin at 349 nm was due to the tryptophan and tyrosine residues. The tryptophan and tyrosine could act as intrinsic fluorescence probes. The chromophores of the tryptophan residues differed from that of the tyrosine residues [26]. The maximum fluorescence intensities of the tryptophan and tyrosine near 280 nm were at about 340 and 300 nm, respectively. If the small molecule could quench the fluorescence of the tryptophan residues, the tryptophan residues should be located near the binding position. The BSA possessed two tryptophan residues (trp-134, trp-213), but the HSA had only single tryptophan residue (trp-214). The quench curves of the BSA and the HSA were similar (Figure 4). The fluorescence intensity was decreased at 340 nm. Thus the studied small molecule should be located or near the tryptophan residues when they were conjugated with the BSA or the HSA.

According to the above mentioned discussions, the HOSalenCo was inserted into the hydrophobic cavities of the BSA and formed the BSA/HOSalenCo conjugation. In the
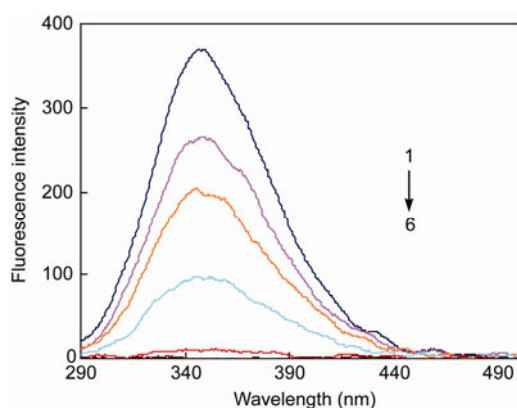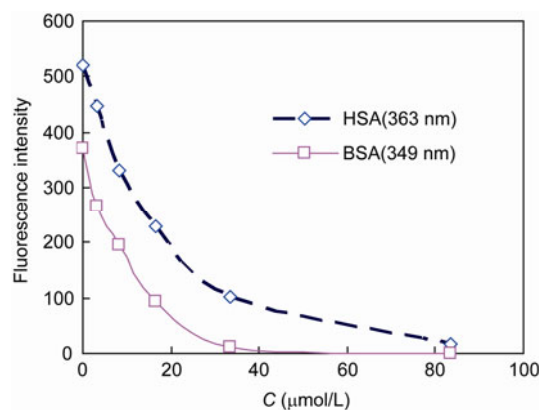

Figure 4   Fluorescence quench curve of HSA and BSA. [HSA]=16.67× 10^{-6} mol/L, [BSA]=16.67×10^{-6} mol/L.

hydrophobic cavities of the BSA, the HOSalenCo made the axial coordination with the amino acid residues. The coordination binding changed the fluorescence characteristics of the tryptophan residues (trp-214). Therefore, the binding site of the HOSalenCo may be first located in the subdomain IIA of the BSA (Figure 5).

2.3   Circular dichroism spectra

The circular dichroism (CD) spectroscopy was used to monitor the change of the α-helical in the BSA (Figure 6). The BSA had a high percentage of α-helical structure which exhibited two negative bands in the ultraviolet region [27]. The intensity of the double peaks reflected the amount of α-helical of the BSA. The Schiff-base complexes did not show any CD signals in this region. The interaction of the BSA and the HOSalenCo could be assessed by following the ellipticity change of the BSA [28]. In the PBS, the BSA showed a maximum negative absorption signal around 216 and 208 nm [29]. Compared with the BSA, the intensity of
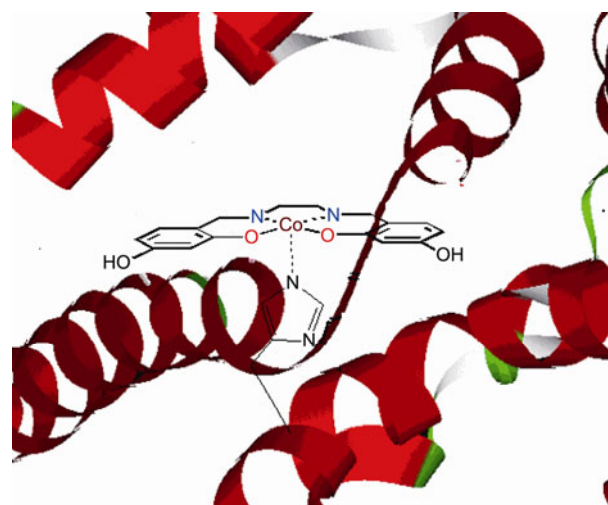

Figure 3   Fluorescence spectra of BSA with adding different concentration of HOSalenCo. (1. [BSA]=16.67×10^{-6} mol/L, 2. [HOSalenCo]=3.28× 10^{-6} mol/L, 3. [HOSalenCo]=8.20×10^{-6} mol/L, 4. [HOSalenCo]=16.67× 10^{-6} mol/L, 5. [HOSalenCo]=33.33×10^{-6} mol/L, 6. [HOSalenCo]=83.33× 10^{-6} mol/L).

Figure 5   Suggested binding site in BSA/HOSalenCo.
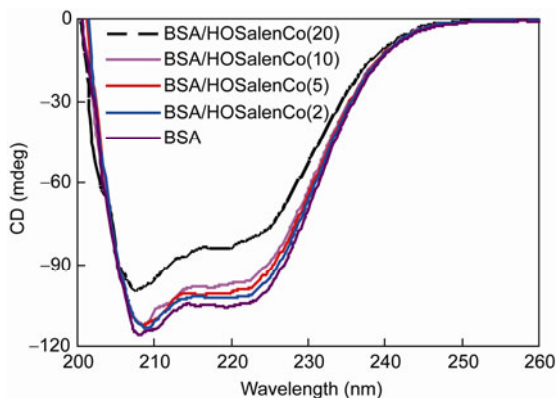
Figure 6　CD spectra of BSA and BSA/HOSalenCo. BSA=1.4×10^{-6} mol/L.

the characteristic CD signal of the BSA/HOSalenCo did not change when the ratio of the HOSalenCo to the BSA was less than 10 (including BSA：HOSalenM=1：2, 1：5 and 1：10) (Figure 6). However the CD signal of the BSA/ HOSalenCo(20) (BSA: HOSalenM=1：20) changed obviously. It indicated that the secondary structure of the BSA was unchanged when the ratio of the HOSalenCo to the BSA was less than 10.

2.4　Native-PAGE

The BSA/HOSalenCo was also studied by the Native-PAGE (Figure 7). The change of molecular weight between the BSA and the BSA/HOSalenCo was slight, so the migration distance of the checking samples depended on their native charges. The results showed that the electrophoretic speeds of the checking samples were similar, but the electrophoresis bands were broadened. The more the Schiff-base metal complexes were integrated, the wider the electrophoresis strips were for the BSA/HOSalenCo. What's more, after the
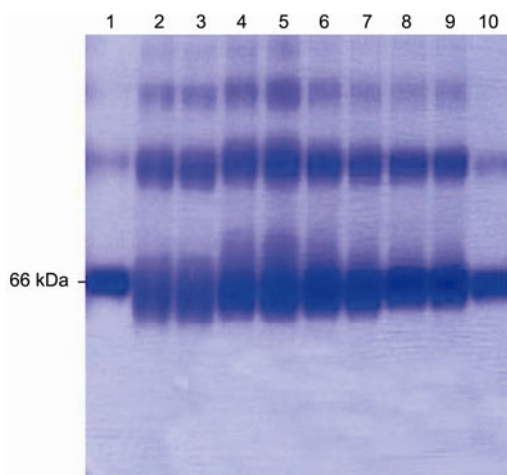

Figure 7　Native-PAGE of BSA and BSA/HOSalenCo. (lines 1, 10: BSA; lines 2, 3: BSA/HOSalenCo(20); lines 4, 5: BSA/ HOSalenCo(10); lines 6, 7: BSA/HOSalenCo(5); lines 8, 9: BSA/HOSalenCo(2).

Schiff-base metal complexes were integrated with the BSA, the enshroud amino acid residues were bared, and the HO-SalenCo changed the charge density of the BSA.

2.5　Hydroxyl radical scavenging ability

The ·OH scavenging activities (Scavenging %) of the BSA/ HOSalenCo with different contents of HOSalenCo were showed in Figure 8. The BSA/HOSalenCo showed an excellent scavenging ·OH activity and was concentration-dependent. The more the HOSalenCo was integrated with the BSA, the better ·OH scavenging activities of the BSA/ HOSalenCo were. With the same inhibitory value, the scavenging value of the BSA/HOSalenCo(20) was much higher than those of other conjugations. The intensities of the scavenging activity of different proportions of the BSA/ HOSalenCo were as follows: BSA/HOSalenCo(20)>BSA/ HOSalenCo(10)>BSA/HOSalenCo(5)>BSA/HOSalenCo (2).

The ·OH scavenging activities of the BSA and the HO-SalenCo were also measured. When the BSA was increased to 0.95 mmol/L, the scavenging effect just reached 41%, and the scavenging activity of the HOSalenCo was very low (Figure 8).

The ·OH scavenging activity of the typical antioxidant, L-ascorbic Acid (Vitamin C), was also measured in the same way. The scavenging effect reached 53% when the VC was added to 0.0058 mmol/L, which was similar to that of BSA/HOSalenCo(20) (Figure 9).

Median extinction concentration (EC_{50}) was an important detection index of the antioxidant activity. It should be a kind of good antioxidants if the tested compound had a low EC_{50}. The EC_{50} values of the BSA, the HOSalenCo and the BSA/HOSalenCo were shown in Table 1. It indicated that the scavenging activity of the BSA drastically increased after being integrated with the HOSalenCo. The more HO-SalenCo was integrated with the BSA, the lower EC_{50} value it had. When the HOSalenCo was integrated with the BSA,
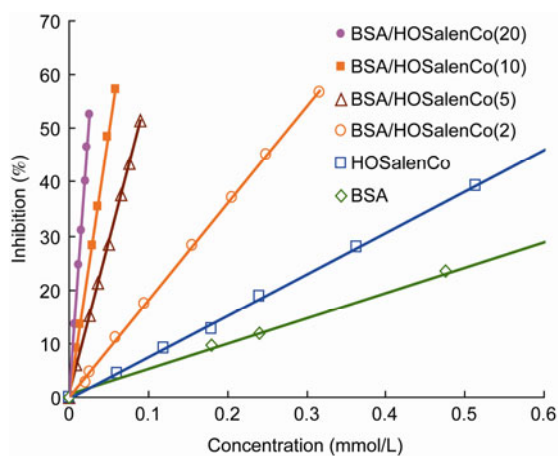

Figure 8　Hydroxyl radical scavenging activity (Scavenging %) of BSA/ HOSalenCo with different ratios of HOSalenCo to BSA.
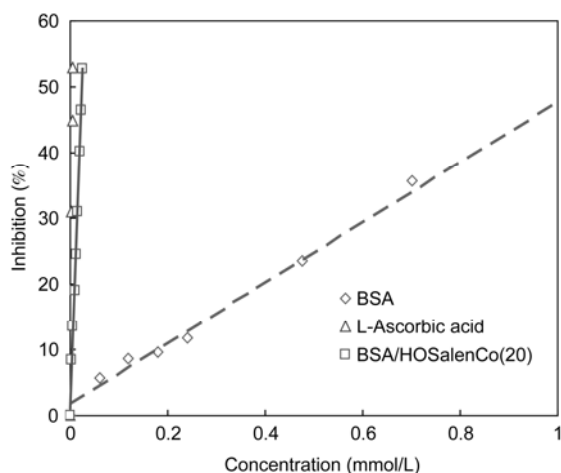
Figure 9   Hydroxyl radical scavenging activity of the BSA/HOSalenCo, BSA and ascorbic acid.

the solubility of the HOSalenCo was improved, and the scavenging activity of the BSA obviously increased. The activity (EC_{50}) of BSA/HOSalenCo(10) (BSA：HOSalenCo= 1：10) was improved by two orders of magnitude compared with the BSA without the HOSalenCo.

The hydroxyl radical scavenging activities of the BSA/ HOSalenMn(20) and the BSA/HOSalenZn(20) were also measured. The scavenging activity of the BSA/HOSalenMn was very low and the BSA/HOSalenZn had no activity.

2.6   Mechanism

Although BSA had an antioxidant activity, its activity was very weak. The HOSalenCo had an antioxidant activity but

it was insoluble in the aqueous solution. With the aim of increasing the antioxidant activity of the BSA and overcoming the infusibility of the HOSalenCo in water, the HOSalenCo and the BSA were conjugated and a new antioxidant conjugation was prepared. The BSA/HOSalenCo showed the excellent activity on the scavenging ·OH. The activity was in a positive correlation with the binding capacity of the HOSalenCo to the BSA. The hydroxyl radical was a briskly radical and had a trend to become a stable ion by accepting or losing an electron. Many literatures have revealed that several charged residues, such as arginine next to the copper(II) ion, can promote the electrostatic steering of the hydroxyl radical substrate to and from the copper ion in the active site [30]. Fridorich showed that M^n was the metalloenzyme in the reduced state and M^{n+1} was the enzyme in the oxidized state. Based on reported catalytic mechanism [24,31], a possible mechanism of the BSA/ HOSalenCo for scavenging ·OH was proposed (Figure 10). Firstly, the metal of the Schiff-base complexes made an axial coordination with the nitrogen atom of the histidine, tryptophan and other amino acid residues of the BSA. Secondly,

Table 1 EC_{50} of the BSA/HOSalenCo and the BSA

Compound	EC_{50} (μmol/L)
BSA/HOSalenCo(20)	25.9
BSA/HOSalenCo(10)	51.0
BSA/HOSalenCo(5)	88.1
BSA/HOSalenCo(2)	233.5
HOSalenCo	650
BSA	1408

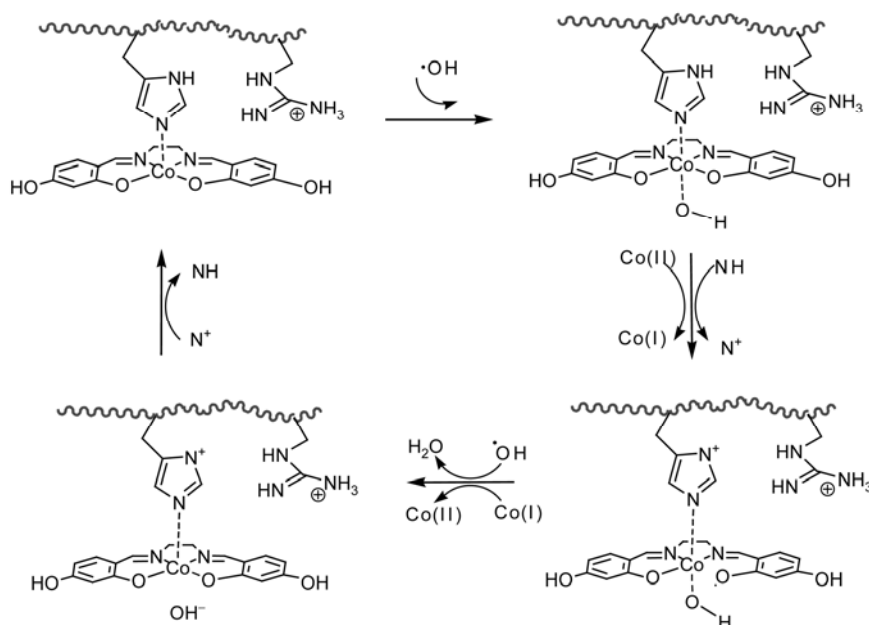**Figure 10**   The mechanism of BSA/HOSalenCo for scavenging hydroxyl radical (·OH).

the hydroxyl radical was attracted by the Co(II) ion under the orienting influence of the guanidyl cation, the hydroxyl radical binding directly to the Co(II) ion. Thirdly, the bound reaction between hydroxyl radical and Co(II) ion changed the electronic cloud distribution of imidazolyl group of histidine. Thus, the hydrogen atom joined with the nitrogen in imidazolyl group was transferred to orbital electron of Co(II), and Co(II) changed to Co(I). So the coordination changed from the planar position to the distorted square pyramid. Fourthly, the change of coordination resulted in the detachment of ·OH from the Co(I). When ·OH was detached, a hydrogen proton from the Co(I) was seized by ·OH. Thus ·OH was quenched to OH⁻ and the Co(I) lost a proton and was changed to the Co(II). Fifthly, when the Co(I) was changed to the Co(II), the coordination was changed from the distorted square pyramid to the planar position, completing a catalytic cycle.

According to the previous studies, the polyphones contribute to the antioxidant activity [32,33]. As is known, there are polyphones in the BSA and HOSalenCo. From the mechanism for ·OH scavenging activity of BSA/HOSalenCo, the excellent hydroxyl radical scavenging activity of the BSA/SalenCo was due to the synergistic action of the polyphenol groups and the coordination reaction. The conjunction of the BSA/SalenCo had an excellent radical scavenging activity when the BSA was bound with small molecule insoluble antioxidants. The BSA had a remarkable ability of binding a wide range of insoluble endogenous and exogenous compounds. Thus the BSA would be a favorable material to study the antioxidant drugs.

3   Conclusions

The biopolymer antioxidant BSA/HOSalenCo with excellent antioxidant activity is prepared via water-soluble protein conjugating with Salen Schiff-base metal complexes. The BSA acts as the bio-consistent carrier and the Schiff-base metal complexes act as the catalyst. After being integrated with the BSA, the insolubility of the HOSalenCo could be well improved. The ·OH scavenging activity of the BSA/HOSalenCo is concentration-dependent. The BSA/HOSalenCo(10) is the best antioxidant because it has an excellent ·OH scavenging activity and the structure of the BSA is kept after the HOSalenCo is integrated with the BSA.

1   Qi H M, Zhang Q B, Zhao T T, et al. Antioxidant activity of different sulfate content derivatives of polysaccharide extracted from *Ulva pertusa* (*Chlorophyta*) *in vitro*. Int J Biol Macromol, 2005, 37: 195–199

2   Koppenol W H. Names for inorganic radicals. Pure Appl Chem, 2000, 72: 437–446

3   Cadenas E, Davies K J A. Mitochondrial free radical generation, oxidative stress and aging. Free Radic Biol Med, 2000, 29: 222–230

4   Liu Y H, Lin Y Sh, Lee T L, et al. Semicarbazide-sensitive amine oxidase inhibitory and hydroxyl radical scavenging activities of aspartic acid β-hydroxamate and glutamic acid γ-monohydroxamate. Botan Stud, 2012, 53: 301–306

5   Nandita S, Rajini P S. Free radical scavenging activity of an aqueous extract of potato peel. Food Chem, 2004, 85: 611–616

6   Shibata T, Ishimaru K, Kawaguchi S, et al. Antioxidant activities of phlorotannins isolated from Japanese Laminariaceae. J Appl Phycol, 2008, 20: 705–711

7   Ohse T, Nagaoka S, Arakawa Y, et al. Cell death by reactive oxygen species generated from water-soluble cationic metalloporphyrins as superoxide dismutase mimics. J Inorg Biochem, 2001, 85: 201–208

8   Vanco J, Svajlenova O, Racanska E, et al. Antiradical activity of different copper (II) Schiff base complexes and their effect on alloxan-induced diabetes. J Trace Elem Med Biol, 2004, 18: 155–161

9   Lacikova L, Muselik J, Masterova I, et al. Antioxidant activity and phenols compounds in different extracts of four *staphylea* L. Species. Molecules, 2007, 12: 98–102

10   Santos M L P, Faljoni-Alario A, Mangrich A S, et al. Ferreira, antioxidant and pro-oxidant properties of some diimine-copper(II) complexes. J Inorg Biochem, 1998, 71: 71–78

11   Tarafder M T H, Kasbollah A, Crouse K A, et al. Synthesis and characterization of Zn(II) and Cd(II) complexes of *S*-benzyl-β-*N*-(2-pyridyl) methylenedithiocarbazate (HNNS): Bioactivity of the HNNS Schiff base and its Zn(II), Cu(II) and Cd(II) complexes and the X-ray structure of the [Zn(NNS)₂] complex. Polyhedron, 2001, 20: 2363–2370

12   Peters T. All About Albumin: Biochemistry Genetics and Medical Applications. San Diego, CA: Academic Press Inc, 1995. 25

13   Peter K, Svend H, Ib J, et al. Albumin binding and time action of acylated insulins in various species. J Pharm Sci, 1995, 312: 725–731

14   Curry S, Madelkow H, Brick P, et al. Crystal structure of human serum albumin complexed with fatty acid reveals an asymmetric distribution of binding sites. Nat Struct Biol, 1998, 5: 827–835

15   Yin X C, Wang R M, He Y F, et al. Artifical oxygen carriers. Prog Chem, 2011, 23: 963–973

16   Gupta P K, Hung C T, Perrier D G. Albumin microspheres, I: Release characteristics of adriamycin. Int J Pharm, 1986: 33: 137–146

17   Brelle M C, Torres-Martinez C L, McNulty J C, et al. Synthesis and characterization of Cu$_x$S nanoparticles. Nature of the infrared band and charge-carrier dynamics. Pure Appl Chem, 2000, 72: 101–117

18   Sheffield W P, Eltringham-Smith L J, Gataiance S, et al. Addition of a sequence from α₂-antiplasmin transforms human serum albumin into a blood clot component that speeds clot lysis. BMC Biotechnol, 2009, 9: 15–21

19   Wang R M, Komatsu T, Nakagawa A, et al. Human serum albumin bearing covalently attached iron(II) porphyrins as O₂-coordination Sites. Bioconjugate Chem, 2005, 15: 23–25

20   Komatsu T, Wang R M, Zunszain P A, et al. Photosensitized reduction of water to hydrogen using human serum albumin complexed with zinc-protoporphyrin IX. J Am Chem Soc, 2006: 128: 16297–16301

21   Moran E C, Kamiguti A S, Cawley J C, et al. Cytoprotective antioxidant activity of serum albumin and autocrine catalase in chronic lymphocytic leukaemia. Br J Haematol, 2002, 116: 316–328

22   Pall T, Benjamin D, Kelly V. Well-defined protein-polymer conjugates—Synthesis and potential applications. Appl Microbiol Biotechnol, 2006, 73: 243–254

23   Pfeiffer P, Breith E, Lubbe E, et al. Tricyclic ortho-condensed partial valence rings. Justus, Liebigs. Ann Chem, 1993, 503: 84–130

24   Yin X C, Li X X, Wang R M, et al. Bifunctional antioxidant enzyme mimics of albumin-binding salphen Schiff-base metal complexes. Pure Appl Chem, 2012, 84: 2641–2652

25 Komatsu T, Ohmichi N, Nakagawa A, et al. O$_2$ and CO binding properties of artificial hemoproteins formed by complexing iron protoporphyrin IX with human serum albumin mutants. J Am Chem Soc, 2005, 127: 15933–15942

26 Boelens R, Sheek R M, Dijkstra K, et al. Sequential assignment of imino- and amino-proton resonances in ^{1}H NMR spectra of oligonucleotides by two-dimensional NMR spectroscopy. Application to a *lac* operator fragment. J Magn Reson, 1985, 62: 378–386

27 Quiming N S, Vergel R B, Nicolas M G, et al. Interaction of bovine serum albumin and metallothionin. J Health Sci, 2005, 51: 8–15

28 Shrivastava H Y, Kanthimathi M, Niar B U. Interaction of Schiff base with bovine serum albumin: Site-specific photocleavage. Biochem Biophys Res Commun, 1999, 265: 311–314

29 Venyaminov S Y, Vasilenko K S. Determination of protein tertiary structure class from circular dichroism spectra. Anal Biochem, 1994, 222: 176–184

30 Zhou Y H, Fu H, Zhao W X, et al. Synthesis, structure and activity of supramolecular mimics for the active site and arg141 residue of copper zinc-superoxide dismutase. Inorg Chem, 2007, 46: 734–739

31 Hart P J, Balbirnie M M, Ogihara N L, et al. Structure-based mechanism for copper-zinc superoxide dismutase. Biochemistry, 1999, 38: 2167–2168

32 Mahfuz E, Omer I, Ibrahim T, et al. Determination of antioxidant activity and antioxidant compounds in wild edible mushrooms. J Food Compos Anal, 2007, 203: 337–345

33 Cai Y Z, Sun M, Xing J, et al. Structure-radical scavenging activity relationships of phenolic compounds from traditional Chinese medicinal plants. Life Sci, 2006, 78: 2872–2888